DOI: 10.1002/chem.201103743

Accelerating the Multifunctionalization of Therapeutic Nanoparticles by Using a Multicomponent Reaction

Hongyu Zhou,[a] Gaoxing Su,[a, b] Peifu Jiao,[a, b] and Bing Yan*[a, b]

The sluggishness of the drug-discovery pipeline in recent decades suggests limitations to the building of many desirable drug properties into a small molecule with a molecular weight of around 500. These desirable properties include at the least anti-disease activity, low toxicity, target selectivity, and optimal absorption, distribution, metabolism and excretion properties. Because of the unique properties of nanoparticles (NPs), including large surface area and flexibility for surface modifications, it is highly feasible to incorporate many drug-like properties into a single nanoparticle.[1,2] Such multifunctionalized nanoparticles (MFNPs) can be equipped with features such as cell targeting, drug delivery, diagnostics, and radiotherapy enhancement. Cancer targeting NPs for drug delivery and radiation enhancement have been reported by others[3–6] and our own laboratory.[7–9] With the use of either a small molecule or protein as targeting moiety, NPs selectively enter cancer cells and enhance killing by both drug action and radiation. Strategies for assembling MFNPs include: 1) multiple functions that are individually attached to NP,[10–12] and 2) multiple functions that are attached to NP with a single attachment point.[13] Modification strategies have been reported for carbon nanotubes,[10–12] quantum dots,[14] gold nanoparticles (GNPs),[15] and supermagnetic NPs.[16,17] However, further applications of both approaches are hindered primarily by the tedious multistep synthesis and the associated difficulties in analytical quality control of each synthesis step. The lack of efficient and well-controlled synthesis approaches to make MFNPs has become a bottleneck limiting the exploration of MFNPs in biological and biomedical applications. Therefore, simpler, faster, more efficient and well-controlled approaches for preparing MFNPs are in urgent need. Here we report a one-step multifunctionalization of nanoparticles employing Ugi multicomponent reaction (MCR).

[a] Dr. H. Zhou, G. Su, P. Jiao, Prof. Dr. B. Yan
Department of Chemical Biology and Therapeutics
St. Jude Children's Research Hospital
Memphis, Tennessee, 38105 (USA)
Fax: (+1) 901-595-5715
E-mail: dr.bingyan@gmail.com

[b] G. Su, P. Jiao, Prof. Dr. B. Yan
School of Chemistry and Chemical Engineering
Shandong University, Jinan, 250100 (P.R. China)

Supporting information for this article is available on the WWW under http://dx.doi.org/10.1002/chem.201103743.

The four starting components for Ugi MCR are thioctic acid, β-cyclodextrin (β-CD), folic acid, and cyclohexyl isocyanide. Thioctic acid serves as a linker to connect the designed multifunctional ligand to GNPs with strong Au–S bonds. The folic acid enables MFNPs to target cancer cells that over-express folate receptor (FR). The isocyanide group is an extra functional group reserved for adding other functions. β-CD is used as the drug carrier because it has been widely used for drug formulation with good biocompatibility.[18] Hydrophobic drugs are easily adsorbed into β-CD's cavity through hydrophobic interactions and are then released at a lower pH. Folic acid functions as the targeting molecule because FR is over-expressed on the surface of several human cancer cells compared to normal cells. MFNPs with folic acid-targeting moieties enter cells through receptor-mediated endocytosis.[19,20] The drug can then be released intracellularly to kill cancer cells. As an additional lethal attack, X-ray irradiation enhanced by GNPs further accelerates cancer cell killing at a dose that is safe to normal cells.[3–9]

Ugi MCRs are powerful tools for building target scaffolds with maximal diversities through a simple reaction process. To make reagents suitable for the Ugi reaction, folic acid was first treated with excess diamines to form an amine, and then one of the hydroxyl groups in β-CD was converted to an aldehyde (detailed information on the synthesis of intermediates is included in the Supporting Information). The Ugi MCR was performed at room temperature in MeOH/DMF with thioctic acid, folic acid-derived amine, β-CD-derived aldehyde, and cyclohexylisocyanide. A similar Ugi product was obtained by using Boc-protected diethylamine to replace folic acid-derived amine and was used as a negative control. The as-synthesized ligands were prepared in mild conditions with high yield through a single step that combined the linker, targeting, and drug-loading functions into one molecule. The ligands were attached to GNPs in situ during the synthesis of multifunctionalized GNPs by treatment with chloroauric acid in the presence of $NaBH_4$. GNPs coupled with Ugi products having either a folic acid group (MFGNP-I) or a Boc group (MFGNP-II) were synthesized. MFGNP-II had the same drug-loading property as MFGNP-I but lacked the targeting capability of MFGNP-I. The anticancer drug doxorubicin (Dox) was loaded onto MFGNP-I and MFGNP-II through noncovalent binding (Scheme 1).

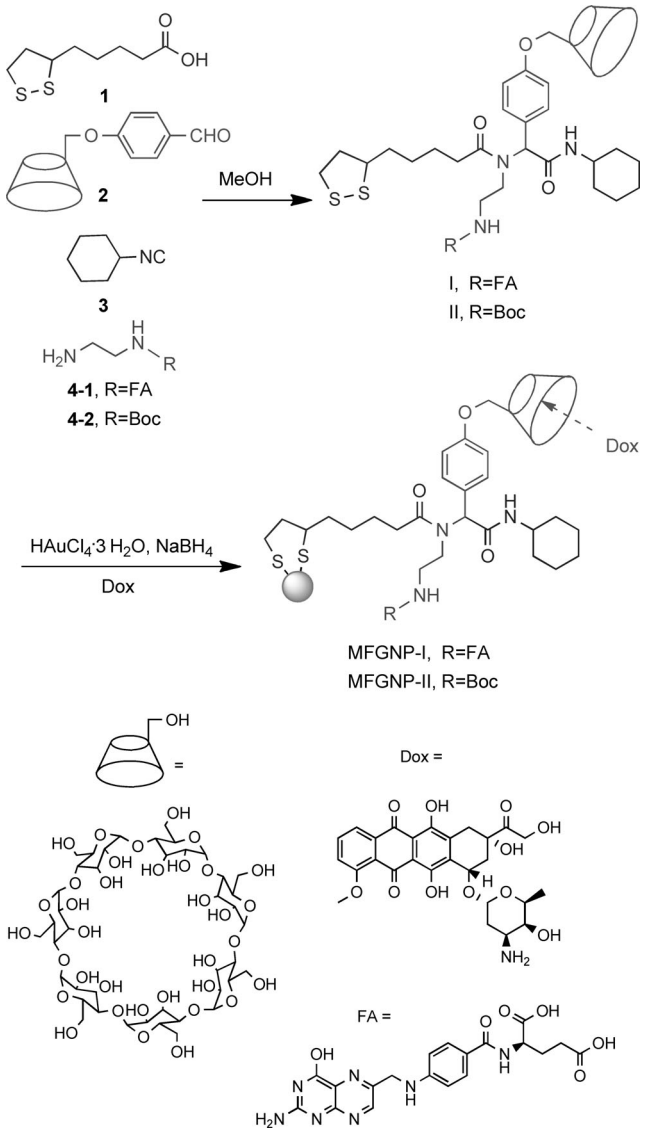

Scheme 1. Scheme of the use of a multicomponent reaction to fabricate multifunctionalized drug-delivery nanosystems.

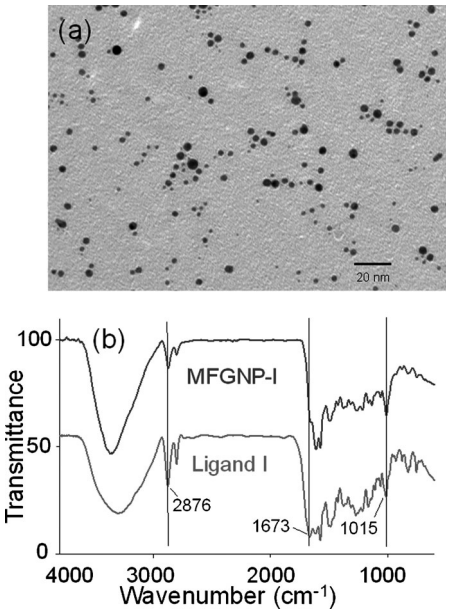

Figure 1. Characterization of multifunctionalized GNPs. a) TEM image of MFGNP-I; scale bar: 20 nm. b) Fourier transform infrared (FTIR) spectra of free ligand I and MFGNP-I obtained by using the KBr pellet method. The FTIR spectrum of MFGNP-I shows similar features to that of ligand I.

GNPs were characterized by a variety of techniques, including transmission electron microscopy (TEM), Fourier transform infrared (FTIR) spectroscopy, UV–visible spectroscopy, ζ potentials, and elemental analysis. TEM images show that the GNPs had an average diameter of 4 nm (Figure 1 a) and dynamic light scattering analyses demonstrate that the particles had a hydrodynamic diameter of 12 nm (Figure S1 in the Supporting Information); this indicates a slight aggregation in aqueous solution. The FTIR spectra of MFGNP-I and -II had similar features as did those of the free ligands (Figure 1 b and Figure S2 in the Supporting Information). Specifically, all spectra contained characteristic C–H stretching vibrations between 2850 and 2950 cm^{-1}, C=O stretching vibrations at 1650 cm^{-1}, and C–O stretching vibrations between 800 and 1200 cm^{-1} (Figure 1 b). When suspended in water, MFGNP-I and -II had ζ potentials of −18 and −24 mV, respectively; this indicates that the electrostatic properties on the surface of these GNPs were similar (Figure S3 in the Supporting Information). Both MFGNP-I and -II had characteristic peaks at approximately 520 nm in UV–visible spectra, which is typical for GNPs. MFGNP-I also showed a peak for folic acid at approximately 270 nm (Figure S4 in the Supporting Information). After analyzing the elemental analysis data to determine the nitrogen content, we concluded that 85 and 132 molecules per nanoparticle were loaded on MFGNP-I and MFGNP-II, respectively (Table S1 in the Supporting Information).

We next explored the drug-loading and -release characteristics of the GNPs. Drug loading was calculated by subtracting the number of Dox molecules remaining in the supernatant after incubating GNPs with Dox for 4 h from the number of Dox molecules initially added to the media. Approximately 50 Dox molecules were loaded onto each GNP. About 23 % of the Dox payloads were released from GNPs within 32 h at pH 7.4. However, more than 70 % of bound Dox was released within 6 h at pH 5.5, a pH value found in endosomes (Figure S5 in the Supporting Information).

To evaluate the cancer cell targeting and killing functions of the GNPs, we performed a series of investigations in cultured cells. HeLa cells are cervical cancer cells that over-express FR. A549 cells, which express very low levels of FR, were used as a negative control. TEM images show that after an 8 h incubation of cells with MFGNP-I, GNP aggregates were prominent in endosome- and lysosome-like vesicles in HeLa cells (Figure 2 a) but rare in A549 cells (Figure 2 b). We then quantitatively determined the cell binding and uptake rates of GNPs by performing inductively coupled plasma mass spectrometry (ICP-MS) analysis.

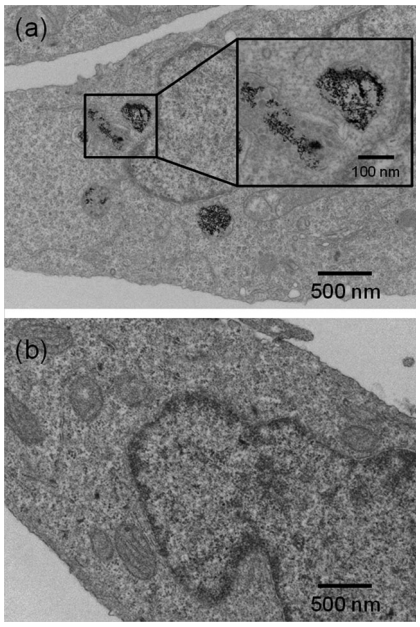

Figure 2. TEM images of: a) HeLa, and b) A549 cells incubated with MFGNP-I for 8 h. The GNP concentration was 50 $\mu g\,mL^{-1}$. GNP aggregates were trapped in organelles, such as the endosome and lysosome, as seen from the magnified section in (a).

MFGNP-II in general showed low rates of cell binding and uptake in both cell lines (Figure 3a), whereas MFGNP-I exhibited a fivefold increase in cell binding and uptake in HeLa cells compared to A549 cells. When compared with

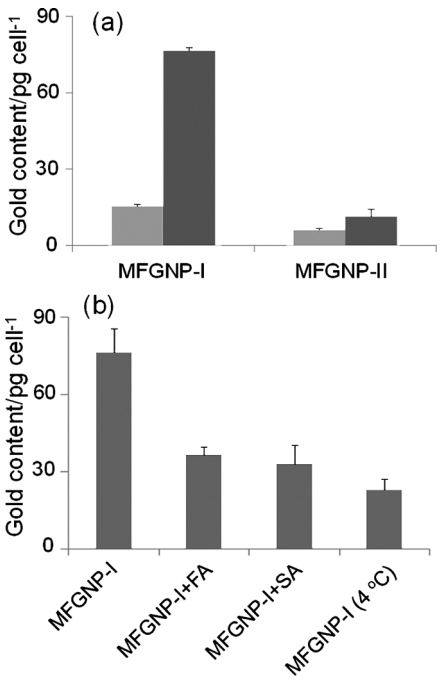

Figure 3. a) Cellular uptake of GNPs was quantitatively determined in HeLa (■; FR positive) and A549 (■; FR negative) cells by performing ICP-MS. b) Cellular uptake of MFGNP-I in HeLa cells under different conditions. The GNP concentration was 50 $\mu g\,mL^{-1}$. The data represent the mean ±standard deviation of the results from three independent experiments. FA: folic acid, SA: sodium azide.

MFGNP-II, MFGNP-I also revealed a sevenfold increase in cell recognition enhancement in HeLa cells (Figure 3a). The data demonstrate that MFGNP-I had a significantly enhanced cell recognition capability in FR positive cells. To test whether folic acid was responsible for the enhanced cell recognition, HeLa cells were pretreated with folic acid and the competing free ligand partially blocked cell binding and uptake (Figure 3b). Cell uptake of MFGNP-I was also partially blocked when HeLa cells were pretreated with sodium azide, a metabolic inhibitor, or incubated with MFGNP-I at 4 °C (Figure 3b); this indicates an energy-dependent endocytosis process. Here we conclude that MFGNP-I achieved cellular delivery through FR-mediated endocytosis.

GNPs have been shown to enhance both X-ray computed tomography (CT)[21,22] and radiation-induced cell death.[23,24] With the confirmation of drug-loading property and cell-recognition enhancement of the MFNPs, we next tested the cell killing induced by the combined drug therapeutic efficacy and X-ray irradiation (Figure 4). At a concentration of

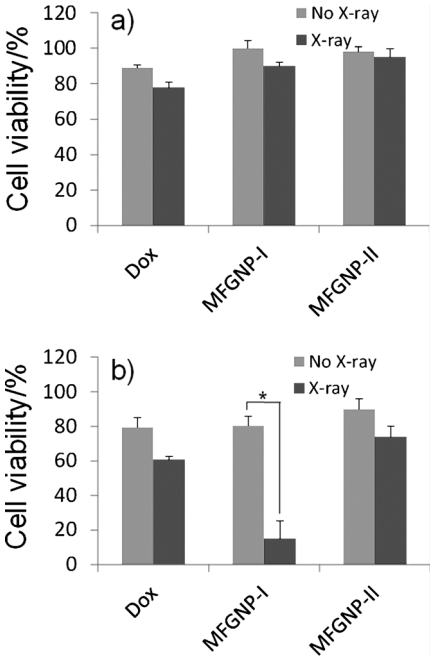

Figure 4. Cell viability of: a) A549, and b) HeLa cells incubated with Dox and GNP–Dox after X-ray irradiation. The Dox concentration for all experiments was 500 nM. The X-ray experiments were performed by using the Minishot X-ray cabinet at 160 kV for a single dose of 5 Gy. The data represent the mean ±standard deviation of the results from three independent experiments; *: $p < 0.05$.

500 nM, Dox induced 11 and 20% cell death in A549 and HeLa cells, respectively. Both MFGNP-I and -II caused low cytotoxicity (i.e., only 2–5% cell death) in A549 cells compared with HeLa cells, because the lack of FR reduced the GNP recognition of A549 cells. MFGNP-I showed a similar toxic profile (21% cell death) whereas MFGNP-II had lower cytotoxicity (10% cell death) in HeLa cells. Following X-ray irradiation, A549 cells treated with either of the

GNPs did not show any clear signs of toxicity. However, with the same dose of X-ray irradiation, HeLa cells treated with MFGNP-I underwent 85% cell death and those treated with MFGNP-II only showed 25% cell death (Figure 4). Our data show that MFGNP-I significantly enhanced cell death; this was caused by the combination of the therapeutic drug and X-ray irradiation in FR positive cells.

In summary, we have demonstrated an accelerated synthesis of a multifunctionalized drug-delivery nanosystem by using Ugi MCR. To our knowledge, this is the first report of the application of MCR in assembling a multifunctionalized nanosystem. The nanosystem enhanced cancer cell targeting selectivity and greatly improved cancer cell killing by combining the effects of the therapeutic drug with those of radiation. We expect that this expedited synthesis method will break the bottleneck for preparation of a wide range of MFNPs for biomedical applications.

Experimental Section

Synthesis of ligand I: FA-Et-NH_2 (**4-1**, 20 mg, 0.05 mmol) was dissolved in MeOH (1 mL). 6-*O*-(4-Formylphenyl)-β-CD (**2**, 40 mg, 0.03 mmol) was dissolved in deionized H_2O (1 mL) and was mixed with the solution of FA-Et-NH_2. The mixture was stirred at room temperature for 1 h. Thioctic acid (15 mg, 0.07 mmol) and 1-isocyanocyclohexane (10 μL, 0.07 mmol) were dissolved in MeOH (1 mL) and added to the mixture in sequence. The resulting solution was stirred at room temperature for 2 days until the completion of the reaction. The mixture was evaporated under vacuum and the final oil was poured into acetone (20 mL). The precipitate was collected by centrifugation at 4000 rpm for 5 min and washed twice with acetone. The crude product was purified by reversed-phase flash chromatography using 20% acetonitrile/water as eluent to give ligand I (31 mg, 43.6%). ^{1}H NMR (400 MHz, [D_6]DMSO with one drop of [D_2]H_2O, 25 °C): δ = 9.85 (s, 1H), 8.69–8.29 (m, 1H), 7.85 (d, J = 8.5 Hz, 2H), 7.72–7.52 (m, 2H), 7.13 (d, J = 8.6 Hz, 2H), 6.96 (d, J = 8.0 Hz, 1H), 6.69–6.52 (m, 1H), 5.79 (m, 1H), 4.95–4.74 (m, 7H), 4.52 (d, J = 31.1 Hz, 1H), 4.27 (d, J = 40.2 Hz, 2H), 3.99 (d, J = 9.6 Hz, 2H), 3.84–3.57 (m, 29H), 3.31 (m, 16H), 3.14 (dt, J = 24.6, 6.0 Hz, 3H), 2.81 (m, 2H), 2.41 (dd, J = 12.7, 6.3 Hz, 2H), 2.20 (t, J = 7.2 Hz, 3H), 1.87 (dq, J = 13.4, 6.5 Hz, 3H), 1.74–1.45 (m, 8H), 1.44–1.25 ppm (m, 6H).

Synthesis of ligand II: Ligand II was synthesized by treatment of **4-2**, 6-*O*-(4-formylphenyl)-β-CD (**2**), thioctic acid, and 1-isocyanocyclohexane according to the procedure described above; yield 56.2%. ^{1}H NMR (400 MHz, [D_4]MeOD, 25 °C): δ = 7.27 (d, J = 8.1 Hz, 2H), 7.01 (d, J = 8.9 Hz, 2H), 5.86 (s, 1H), 4.96 (m, 7H), 4.57 (m, 7H), 4.26–4.03 (m, 2H), 3.90–3.65 (m, 23H), 3.65–3.37 (m, 15H), 3.25–2.98 (m, 3H), 2.70–2.40 (m, 3H), 1.98–1.58 (m, 8H), 1.47 (s, 9H), 1.46–1.10 ppm (m, 6H).

Synthesis of multifunctionalized GNPs: In a typical experiment, water (1.0 mL) containing chloroauric acid (15.0 mg, 0.038 mmol) was added to a solution of either ligand I or II (15.0 mg) in water (8.0 mL). After being stirred for 15 min at room temperature, $NaBH_4$ (6.0 mg, 0.15 mmol) in water (6.0 mL) was added to the mixture dropwise. The solution turned red immediately and was stirred for 4 h at room temperature. HCl (1N) was added to the reaction mixture dropwise to neutralize the excess sodium tetrahydroborate until the pH reached 7.0. To remove the free ligand from the nanoparticles, the reaction mixture was centrifuged at 4000 rpm for 30 min with Millipore centrifugal filters with molecule weight cut-off 10 k (50 mL tube). The colorless supernatant was decanted and the solid was dissolved in deionized water (10 mL) and centrifuged again at 4000 rpm for 30 min. This wash/centrifugation cycle was repeated five times. After the final washing step, the GNPs were dissolved in Millipore water (5–10 mL) and used as stock solution. The gold concentration of the stock solution was determined by ICP-MS method.

Characterization: TEM images of GNPs were taken by using a JEOL 1200 EX transmission electron microscope (JEOL, Tokyo, Japan) at 80 kV. The images were acquired by using an AMT 2k CCD camera. The dynamic diameter of the GNPs was measured by using the Dynapro Titan system (Wyatt Technology, Santa Barbara, CA). FTIR spectra were recorded on a Nicolet 6700 FT-IR spectrometer (Thermo Scientific). The stock solution (3.0 mL) was dried under vacuum by using GeneVac solvent evaporator. The dry samples were collected for FTIR analysis. Then ζ potentials of GNPs were measured in a Malvern Nano Z Zetasizer. GNPs were suspended in water. Each material was tested three times. The UV/Vis absorption spectra of the GNPs were obtained with a Varian 5000 UV/Vis spectrometry (Varian, Santa Clara, CA). All the spectra had subtracted background with baseline correction by the absorption of deionized water. The MFGNPs used for characterization and following cellular uptake experiments did not contain Dox.

Cell culture: HeLa cells were grown in Eagle's minimum essential medium (MEM, Invitrogen, IL). A549 cells were grown in RPMI 1640 (Gibco, Invitrogen, IL). Each cell culture medium was supplemented with fetal bovine serum (FBS, 10%), penicillin (10 U mL^{-1}) and streptomycin (10 mg mL^{-1}).

TEM experiments with cells: TEM images of cells were taken by using a JEOL 1200 EX transmission electron microscope (JEOL, Tokyo, Japan) at 80 kV. The images were acquired by using an AMT 2k CCD camera. To obtain the TEM images, both cell lines were cultured in 6-well plates with a density of 100000 cells per well. Cultures were incubated at 37 °C under a humidified atmosphere with CO_2 (5%). After 24 h incubation, old medium was removed and fresh medium containing GNPs (50 μg mL^{-1}) was added. The cells were incubated with GNPs for 8 h and washed three times with cold PBS to remove unbound GNPs. The cells were fixed with glutaraldehyde (2.5%) in Na-cacodylate buffer (0.1 M, Tousimis Research Corporation) for 30 min at room temperature. The fixed cells were collected for TEM study.

Cellular uptake of GNPs: Both cell lines were cultured in 12-well plates with a density of 50000 cells per well. Cultures were maintained at 37 °C under a humidified atmosphere with CO_2 (5%). After 24 h incubation, the cells were washed once with cold PBS, and the solutions of GNPs (50 μg mL^{-1}) were added. The cells were incubated with GNPs for 8 h and then washed three times with cold PBS to remove unbound GNPs. The cells were detached with trypsin-EDTA solution (0.25% trypsin, 1 mM EDTA). The detached cells were counted by using Cellometer cell counter Auto T4 (Nexcelom Bioscience, Lawrence, MA) and then prepared for ICP-MS. Each experiment was repeated three times.

ICP-MS sample preparation and measurements: All ICP-MS measurements were performed on a Varian 820. GNPs were incubated with different cell lines separately, as described above. After detaching and counting the cells, the resulting cell lysate (100 μL) was digested for 4 h at 37 °C by adding Aqua Regia (200 μL). The solution (50 μL) was diluted to 5.0 mL with a ^{209}Bi internal standard (50 ppb) solution in HNO_3 (1.0%) and used for ICP-MS measurements. Cellular uptake experiments with each GNP were repeated three times, and each replicate was measured five times by ICP-MS. A series of gold standard solutions (1000, 500, 100, 50, 10, 5, and 1 ppb) with ^{209}Bi internal standard (50 ppb) were prepared before each measurement. The resulting calibration curve was used to calculate the gold concentration taken up by the different cell lines. Two injections of ^{209}Bi internal standard solution in HNO_3 were used to wash the instrument between analyses to remove trace amounts of gold.

X-ray irradiation: Cells were cultured in 96-well plates with a density of 5000 cells per well. After 24 h incubation, the cells were washed once with cold PBS. Dox and GNP–Dox solutions were added with a specified final Dox concentration (500 nM). The cells were incubated for 8 h and then washed three times with cold PBS to remove unbound GNPs. Fresh medium (100 μL) was then added to the plates. The AXR Minishot 160 X-ray cabinet irradiator working with 1 mm aluminum at 160 kV and 3 mA, and yielding a mean dose rate of 27.0 R min^{-1} was used for X-ray irradiation. The cells were exposed to X-ray irradiation with a total dose of 5 Gy; this corresponds to an irradiation time of 18.5 min. The XTT measurements were performed 48 h after X-ray irradiation to test cell vi-

ability. For all experiments, a duplicate 96-well plate treated identically but without X-ray irradiation was used as control. Each experiment was performed three times.

Cytotoxicity assay: Cell proliferation kit II (XTT, Roche Diagnostics Corporation, Indianapolis, IN) was used to evaluate the viability of the cells after uptake of GNPs and X-ray irradiations. The assay is based on the cleavage of the water-soluble yellow tetrazolium salt XTT to form an orange formazan dye by metabolically active cells. The formazan was directly quantified by using a microplate reader, and correlated with the number of viable cells. Suspension medium was removed 48 h after the X-ray irradiation and XTT solution (50 μL, 1 mg mL^{-1}, Sigma) and fresh medium (100 μL) were added to each well and incubated at 37 °C for 4 h. The absorbance of all samples was measured at 480 and 650 nm separately by using a SpectraMax M5 microplate reader (Molecular Devices Sunnyvale, CA) and the cell viability was calculated following the standard procedure. Each experiment was performed three times.

Acknowledgements

We thank Sharon Frase and Linda Mann for technical assistance, and Cherise M. Guess for editing assistance. This work was supported by the National Basic Research Program of China (2010CB933504), National Natural Science Foundation of China (90913006, 21077068, and 21137002), National Cancer Institute (P30A027165), and the American Lebanese Syrian Associated Charities (ALSAC).

Keywords: drug delivery · multicomponent reactions · multifunctionalization · nanoparticles · X-ray irradiation

[1] M. Ferrari, *Nat. Rev. Cancer* **2005**, *5*, 161–171.
[2] V. P. Torchilin, *Adv. Drug Delivery Rev.* **2006**, *58*, 1532–1555.
[3] T. Kong, J. Zeng, X. Wang, X. Yang, J. Yang, S. McQuarrie, A. McEwan, W. Roa, J. Chen, J. Z. Xing, *Small* **2008**, *4*, 1537–1543.
[4] N. Chattopadhyay, Z. Cai, J.-P. Pignol, B. Keller, E. Lechtman, R. Bendayan, R. M. Reilly, *Mol. Pharm.* **2010**, *7*, 2194–2206.
[5] P. Huang, L. Bao, C. Zhang, J. Lin, T. Luo, D. Yang, M. He, Z. Li, G. Gao, B. Gao, S. Fu, D. Cui, *Biomaterials* **2011**, *32*, 9796–9809.
[6] Y.-A. Shieh, S.-J. Yang, M.-F. Wei, M.-J. Shieh, *ACS Nano* **2010**, *4*, 1433–1442.
[7] H. Zhou, P. Jiao, L. Yang, X. Li, B. Yan, *J. Am. Chem. Soc.* **2011**, *133*, 680–682.
[8] P. Jiao, H. Zhou, M. Otto, Q. Mu, L. Li, G. Su, Y. Zhang, E. R. Butch, S. E. Snyder, G. Jiang, B. Yan, *J. Am. Chem. Soc.* **2011**, *133*, 13918–13921.
[9] X. Li, H. Zhou, L. Yang, G. Du, A. S. Pai-Panandiker, X. Huang, B. Yan, *Biomaterials* **2011**, *32*, 2540–2545.
[10] J. Chen, S. Chen, X. Zhao, L. V. Kuznetsova, S. S. Wong, I. Ojima, *J. Am. Chem. Soc.* **2008**, *130*, 16778–16785.
[11] G. Pastorin, W. Wu, S. Wieckowski, J. P. Briand, K. Kostarelos, M. Prato, A. Bianco, *Chem. Commun.* **2006**, 1182–1184.
[12] W. Wu, S. Wieckowski, G. Pastorin, M. Benincasa, C. Klumpp, J. P. Briand, R. Gennaro, M. Prato, A. Bianco, *Angew. Chem.* **2005**, *117*, 6516–6520; *Angew. Chem. Int. Ed.* **2005**, *44*, 6358–6362.
[13] E. Garanger, E. Aikawa, F. Reynolds, R. Weissleder, L. Josephson, *Chem. Commun.* **2008**, 4792–4794.
[14] X. H. Gao, Y. Y. Cui, R. M. Levenson, L. W. K. Chung, S. M. Nie, *Nat. Biotechnol.* **2004**, *22*, 969–976.
[15] S. Kumar, J. Aaron, K. Sokolov, *Nat. Protoc.* **2008**, *3*, 314–320.
[16] M. Liong, J. Lu, M. Kovochich, T. Xia, S. G. Ruehm, A. E. Nel, F. Tamanoi, J. I. Zink, *ACS Nano* **2008**, *2*, 889–896.
[17] R. Weissleder, K. Kelly, E. Y. Sun, T. Shtatland, L. Josephson, *Nat. Biotechnol.* **2005**, *23*, 1418–1423.
[18] M. E. Davis, M. E. Brewster, *Nat. Rev. Drug Discovery* **2004**, *3*, 1023–1035.
[19] P. S. Low, A. C. Antony, *Adv. Drug Delivery Rev.* **2004**, *56*, 1055–1058.
[20] R. J. Lee, P. S. Low, *J. Biol. Chem.* **1994**, *269*, 3198–3204.
[21] W. Eck, A. I. Nicholson, H. Zentgraf, W. Semmler, S. Bartling, *Nano Lett.* **2010**, *10*, 2318–2322.
[22] R. Popovtzer, A. Agrawal, N. A. Kotov, A. Popovtzer, J. Balter, T. E. Carey, R. Kopelman, *Nano Lett.* **2008**, *8*, 4593–4596.
[23] T. Kong, J. Zeng, X. P. Wang, X. Y. Yang, J. Yang, S. McQuarrie, A. McEwan, W. Roa, J. Chen, J. Z. Xing, *Small* **2008**, *4*, 1537–1543.
[24] C. J. Liu, C. H. Wang, S. T. Chen, H. H. Chen, W. H. Leng, C. C. Chien, C. L. Wang, I. M. Kempson, Y. Hwu, T. C. Lai, M. Hsiao, C. S. Yang, Y. J. Chen, G. Margaritondo, *Phys. Med. Biol.* **2010**, *55*, 931–945.

Received: November 28, 2011
Published online: March 21, 2012

